Inorg. Chem. **2002**, *41*, 4788–4797

Peroxynitrite Decomposition Activity of Iron Porphyrin Complexes

Michael P. Jensen*,† and Dennis P. Riley‡

Monsanto Corporate Research,§ 800 North Lindbergh Boulevard, St. Louis, Missouri 63167

Received October 22, 2001

Peroxynitrite ($ONOO^-$/ONOOH), a putative cytotoxin formed by combination of nitric oxide ($NO^\bullet$) and superoxide ($HO_2^\bullet$) radicals, is decomposed catalytically by micromolar concentrations of water-soluble Fe(III) porphyrin complexes, including 5,10,15,20-tetrakis(2′,4′,6′-trimethyl-3,5-disulfonatophenyl)porphyrinatoferrate(7–), Fe(TMPS); 5,10,15,20-tetrakis(4′-sulfonatophenyl)porphyrinatoiron(3–), Fe(TPPS); and 5,10,15,20-tetrakis(*N*-methyl-4′-pyridyl) porphyrinatoiron(5+), Fe(TMPyP). Spectroscopic (UV–visible), kinetic (stopped-flow), and product (ion chromatography) studies reveal that the catalyzed reaction is a net isomerization of peroxynitrite to nitrate (NO_3^-). One-electron catalyst oxidation forms an oxoFe(IV) intermediate and nitrogen dioxide, and recombination of these species is proposed to regenerate peroxynitrite or to yield nitrate. Michaelis–Menten kinetics are maintained accordingly over an initial peroxynitrite concentration range of 40–610 μM at 5.0 μM catalyst concentrations, with K_m in the range 370–620 μM and limiting turnover rates in the range of 200–600 s^{-1}. Control experiments indicate that nitrite is not a kinetically competent reductant toward the oxidized intermediates, thus ruling out a significant role for $NO_2^\bullet$ hydrolysis in catalyst turnover. However, ascorbic acid can intercept the catalytic intermediates, thus directing product distributions toward nitrite and accelerating catalysis to the oxidation limit. Additional mechanistic details are proposed on the basis of these and various other kinetic observations, specifically including rate effects of catalyst and peroxynitrite concentrations, solution pH, and isotopic composition.

Introduction

Peroxynitrite is a highly reactive oxidant that is generated by the combination of nitric oxide ($NO^\bullet$) and superoxide ($O_2^{-\bullet}$) radicals[1,2] and is considered to be a possible mediator of nitric oxide biochemistry and oxidative stress injury.[3] Although the peroxynitrite anion ($ONOO^-$) is stable indefinitely, facile protonation forms highly reactive peroxynitrous acid (ONOOH).[4] Many biologically important molecules react with the acid form of peroxynitrite to form products akin to those of hydroxyl ($HO^\bullet$) and nitrogen dioxide ($NO_2^\bullet$) radicals.[5] Among the deleterious biological effects attributed to this chemistry are DNA strand cleavage,[6] lipid peroxidation,[7] protein nitration,[8] enzyme inactivation,[9,10] and release of free metal ions.[10] These may contribute to cell death and tissue injury through oxidative stress and thus promote a number of disease states.[11]

* To whom correspondence should be addressed: e-mail jensen@chem.umn.edu.

† Present address: Department of Chemistry, 207 Pleasant St. SE, University of Minnesota, Minneapolis, MN 55455.

‡ Present address: MetaPhore Pharmaceuticals, 1910 Innerbelt Business Center Dr., St. Louis, MO 63114.

§ Monsanto merged with Pharmacia and Upjohn in April 2000 to form Pharmacia Corp.

(1) The term "peroxynitrite" is used herein to designate the equilibrium mixture of peroxynitrite anion ($ONOO^-$) and peroxynitrous acid (ONOOH). Specific reference is made to either species in the conjugate acid−base pair when exclusive consideration is required. The systematic name of peroxynitrite anion is oxoperoxonitrate(1−). The systematic name of $NO^\bullet$ ("nitric oxide") is nitrogen monoxide. Abbrevations used: Fe(TMPyP), 5,10,15,20-tetrakis(*N*-methyl-4′-pyridyl)porphyrinatoiron(5+); Fe(TPPS), 5,10,15,20-tetrakis(4′-sulfonatophenyl)porphyrinatoferrate (3−); Fe(TMPS), 5,10,15,20-tetrakis(2′,4′,6′-trimethyl-3,5-disulfonatophenyl)porphyrinatoferrate(7−); *m*-CPBA, *m*-chloroperoxybenzoic acid.

(2) (a) Blough, N. V.; Zafiriou, O. C. *Inorg. Chem.* **1985**, *24*, 3502. (b) Huie, R. E.; Padmaja, S. *Free Radical Res. Commun.* **1993**, *18*, 195.

(3) (a) Edwards, J. O.; Plumb, R. C. *Prog. Inorg. Chem.* **1993**, *41*, 599. (b) Pryor, W. A.; Squadrito, G. L. *Am. J. Physiol.* **1995**, *268*, L699.

(4) (a) Anbar, M.; Taube, H. *J. Am. Chem. Soc.* **1954**, *76*, 6243. (b) Halfpenny, E.; Robinson, P. L. *J. Chem. Soc.* **1952**, 928 and 939.

(5) (a) Koppenol, W. H.; Kissner, R. *Chem. Res. Toxicol.* **1998**, *11*, 87. (b) Merenyi, G. Lind, J. *Chem. Res. Toxicol.* **1998**, *11*, 243. (c) Coddington, J. W.; Hurst, J. K.; Lymar, S. V. *J. Am. Chem. Soc.* **1999**, *121*, 2438.

(6) King, P. A.; Anderson, V. E.; Edwards, J. O.; Gustafson, G.; Plumb, R. C.; Suggs, J. W. *J. Am. Chem. Soc.* **1992**, *114*, 5430.

(7) Radi, R.; Beckman, J. S.; Bush, K. M.; Freeman, B. A. *Arch. Biochem. Biophys.* **1991**, *288*, 481.

(8) Crow, J. P.; Ischiropoulous, H. *Methods Enzymol.* **1996**, *269*, 175.

(9) (a) Schmidt, K.; Klatt, P.; Mayer, B. *Biochem J.* **1994**, *361*, 645. (b) Huehmer, A. F. R.; Nishida, C. R.; Ortiz de Montellano, P. R.; Schoeneich, C. *J. Biol. Chem.* **1994**, *269*, 29405. (c) MacMillan-Crow, L. A.; Crow, J. P.; Kerby, J. D.; Beckman, J. S.; Thompson, J. A. *Proc. Natl. Acad. Sci. U.S.A.* **1996**, *93*, 11853.

(10) (a) Hausladen, A.; Fridovich, I. *J. Biol. Chem.* **1994**, *269*, 29405. (b) Castro, L.; Rodriguez, M.; Radi, R. *J. Biol. Chem.* **1994**, *269*, 29409.

10.1021/ic011089s CCC: $22.00
Published on Web 08/14/2002

We reported that water-soluble Fe(III) porphyrin complexes catalyze rapid isomerization of peroxynitrite to nitrate (NO_3^-) under physiologically relevant conditions (pH 7.4, 37 °C).[12] Heme peroxidases are oxidized by peroxynitrite,[13] and this reactivity supports peroxynitritase catalysis.[14] Other reports of peroxynitrite reduction and isomerization catalysis by heme proteins,[15] metalloporphyrins,[16] and related complexes also have appeared.[17] Some of these complexes were found to have significant effects in pharmacological models of oxidative disease states.[18]

Given the continuing interest in these various peroxynitrite decomposition reactivities, we now provide a full report of the kinetics of peroxynitrite decomposition catalysis afforded by water-soluble Fe(III) porphyrins.

Experimental Section

Materials. Water used in synthetic and analytical solutions was deionized and doubly distilled, first off permanganate, under a nitrogen atmosphere, except for deuterium oxide (99.9% D), which was used as received from Aldrich. Buffers were prepared from reagent-grade phosphate salts (Aldrich) and NaOH (Baker) and kept in sealed containers. Carbonate levels in month-old buffer solutions measured after extensive use were found to be <10 ppm. pH measurements were made against standard buffers (VWR) with an Orion 320 pH meter. A correction of 0.41 was added to pH meter readings to obtain pD values in D_2O.[19]

Peroxynitrite was synthesized in 80−100% spectrophotometric yields by nucleophilic displacement of ethoxyethanol from ethoxyethylnitrite by hydrogen peroxide in 0.3 N NaOH, according to published procedures.[20] Base hydrolysis of ethoxyethylnitrite is known to compete with peroxynitrite formation,[20] and the product solutions accordingly contain residual ethoxyethanol (<1.3 equiv), nitrite (<0.3 equiv), and hydrogen peroxide (<0.3 equiv). Peroxynitrite anion concentrations were assessed by UV−visible spectrophotometry, $\epsilon_{302nm} = 1670\ M^{-1}\ cm^{-1}$.[21] Stocks were kept sealed and frozen up to 1 month until use and were discarded upon significant decomposition.

Concentrated ascorbate (Aldrich) stocks were freshly prepared in pure water, kept on ice, and added to buffers just prior to sample analysis to minimize aerobic catalyst bleachings; control stocks were monitored by UV−visible spectroscopy to establish that autoxidation was negligibly slow on the laboratory time scale.

Crude *m*-chloroperoxybenzoic acid (*m*-CPBA, Aldrich) was slurried in pH 7.4 buffer overnight, recovered by filtration, dried to constant weight, and stored in a freezer. Stock solutions were prepared by dissolution of the acid-free solid in a minimum amount of methanol, followed by dilution with pH 10.4 phosphate buffer.

Fe(TMPyP) and Fe(TPPS) were purchased from Porphyrin Products as the tetratosylate and tetrasodium salts, respectively, of the monochloride complexes. Fe(TMPS) was prepared from tetramesitylporphine (Porphyrin Products) and isolated as the octasodium salt of the monochloride complex by a published procedure.[22]

Kinetic Measurements. Catalyst solutions in 0.10−0.30 M phosphate buffers were mixed with alkaline $ONOO^-$ in stopped flow, UV−visible, dual-beam spectrophotometers. The adequacy of the buffer capacity was confirmed in control experiments. OLIS RSM-1000 and Hi-Tech SF-61 DX-2 instruments were utilized in this study. The configurations of both instruments permitted continuous flow of water from thermostated baths over the flow path and firing syringes containing the reagents, and the temperature was maintained at 37.0(1) °C.

Peroxynitrite decay was monitored near 302 nm. First-order decay rates were fitted by standard techniques with software provided by the instrument manufacturers. Michaelis−Menten data were obtained by linear fits over the first 25% of the reaction and were corrected for background decay by similar fits to data recorded in the absence of catalyst. Least-squares regressions were calculated with SigmaPlot, v. 4.00 (1997, SPSS Inc.).

Product Ion Measurements. Product distributions were determined in triplicate by ion chromatographic measurements. Blind measurements were performed by Kyle Huang and Dr. Dutt

(11) Beckman, J. S.; Beckman, T. W.; Chen, J.; Marshall, P. A.; Freeman, B. A. *Proc. Natl. Acad. Sci. U.S.A.* **1990**, *87*, 1620.

(12) (a) Stern, M. K.; Salvemini, D. *PCT Int. Appl*., WO95/31197, 1995. (b) Stern, M. K.; Jensen, M. P.; Kramer, K. *J. Am. Chem. Soc*. **1996**, *118*, 8735.

(13) Floris, R.; Piersma, S. R.; Yang, G.; Jones, P.; Wever, R. *Eur. J. Biochem*. **1993**, *215*, 767.

(14) (a) Wengenack, N. L.; Jensen, M. P.; Rusnak, F.; Stern, M. K. *Biochem. Biophys. Res. Commun.* **1999**, *256*, 485. (b) Jensen, M. P.; Riley, D. P. Manuscript in preparation.

(15) (a) Landino, L. M.; Crews, B. C.; Timmons, M. D.; Morrow, J. D.; Marnett, L. J. *Proc. Natl. Acad. Sci. U.S.A.* **1996**, *93*, 15069. (b) Alayash, A. I.; Brockner Ryan, B. A.; Cashon, R. E. *Arch. Biochem. Biophys*. **1998**, *349*, 65. (c) Mehl, M.; Daiber, A.; Herold, S.; Shoun, H.; Ullrich, V. *Nitric Oxide* **1999**, *3*, 142. (d) Pearce, L. L.; Pitt, B. R.; Peterson, J. *J. Biol. Chem*. **1999**, *274*, 35763. (e) Goodwin, D. C.; Landino, L. M.; Marnett, L. J. *FASEB J*. **1999**, *13*, 1121. (f) Zou, M.-H.; Daiber, A.; Peterson, J. A.; Shoun, H.; Ullrich, V. *Arch. Biochem. Biophys*. **2000**, *376*, 149. (g) Minetti, M.; Pietraforte, D.; Carbone, V.; Salzano, A. M.; Scorza, G.; Marino, G. *Biochemistry* **2000**, *39*, 6689. (h) Exner, M.; Herold, S. *Chem. Res. Toxicol*. **2000**, *13*, 287. (i) Daiber, A.; Herold, S.; Schoeneich, C.; Namgaladze, D.; Peterson, J. A.; Ullrich, V. *Eur. J. Biochem.* **2000**, *267*, 6729. (j) Herold, S.; Matsui, T.; Watanabe, Y. *J. Am. Chem. Soc*. **2001**, *123*, 4085. (k) Bourassa, J. L.; Ives, E. P.; Marqueling, A. L.; Shimanovich, R.; Groves, J. T. *J. Am. Chem. Soc*. **2001**, *123*, 5142.

(16) (a) Groves, J. T.; Marla, S. S. *J. Am. Chem. Soc*. **1995**, *117*, 9578. (b) Lee, J.; Hunt, J. A.; Groves, J. T. *Bioorg. Med. Chem. Lett*. **1997**, *7*, 2913. (c) Balavoine, G. G. A.; Geletii, Y. V.; Bejan, D. *Nitric Oxide* **1997**, *1*, 507. (d) Hunt, J. A.; Lee, J.; Groves, J. T. *Chem. Biol*. **1997**, *4*, 845. (e) Marla, S. S.; Lee, J.; Groves, J. T. *Proc. Natl. Acad. Sci. U.S.A.* **1997**, *94*, 14243. (f) Lee, J.; Hunt, J. A.; Groves, J. T. *J. Am. Chem. Soc*. **1998**, *120*, 6053. (g) Lee, J.; Hunt, J. A.; Groves, J. T. *J. Am. Chem. Soc.* **1998**, *120*, 7493. (h) Ferrer-Sueta, G.; Batinic-Haberle, I.; Spasojevic, I.; Fridovich, I.; Radi, R. *Chem. Res. Toxicol*. **1999**, *12*, 442. (i) Crow, J. P. *Arch. Biochem. Biophys*. **1999**, *371*, 41. (j) Shimanovich, R.; Groves, J. T. *Arch. Biochem. Biophys*. **2001**, *387*, 307.

(17) (a) Riley, D. P.; Busch, D. H.; Zhang, X. *PCT Int. Appl*. WO98−US5567, 1998. (b) Zhang, X.; Busch, D. H. *J. Am. Chem. Soc*. **2000**, *122*, 1229. (c) Groves, J. T.; Moeller, S. M. *PCT Int. Appl*. WO2000−075144, 2000. (d) Shimanovich, R.; Hannah, S.; Lynch, S.; Gerasimchuck, N.; Mody, T. D.; Magda, D.; Sessler, J.; Groves, J. T. *J. Am. Chem. Soc*. **2001**, *123*, 3613.

(18) (a) Salvemini, D.; Wang, Z.-Q.; Bourdon, D. M.; Stern, M. K.; Currie, M. G.; Manning, P. T. *Eur. J. Pharmacol*. **1996**, *303*, 217. (b) Szabo, C.; Day, B. J.; Salzman, A. L. *FEBS Lett*. **1996**, *381*, 82. (c) Zingarelli, B.; Day, B. J.; Crapo, J. D.; Salzman, A. L.; Szabo, C. *Br. J. Pharmacol.* **1997**, *120*, 259. (d) Salvemini, D.; Wang, Z.-Q.; Stern, M. K.; Currie, M. G.; Misko, T. P. *Proc. Natl. Acad. Sci. U.S.A.* **1998**, *95*, 2659. (e) Misko, T. P.; Highkin, M. K.; Veenhuizen, A. W.; Manning, P. T.; Stern, M. K.; Currie, M. G.; Salvemini, D. *J. Biol. Chem*. **1998**, *273*, 15646. (f) Salvemini, D.; Riley, D. P.; Lennon, P. J.; Wang, Z.-Q.; Currie, M. G.; Macarthur, H.; Misko, T. P. *Br. J. Pharmacol*. **1999**, *127*, 685. (g) Cross, A. H.; San, M.; Stern, M. K.; Keeling, R. M.; Salvemini, D.; Misko, T. P. *J. Neuroimmunol*. **2000**, *107*, 21. (h) Cuzzocrea, S.; Misko, T. P.; Costantino, G.; Mazzon, E.; Micali, A.; Caputi, A. P.; Macarthur, H.; Salvemini, D. *FASEB J*. **2000**, *14*, 1061. (i) Choi, I. Y.; Lee, S. J.; Nam, W.; Park, J.-S.; Ko, K. H.; Kim, H.-C.; Shin, C. Y.; Chung, J.-H.; Noh, S. K.; Choi, C.-R.; Shin, D.-H.; Kim, W.-K. *J. Neuroimmunol*. **2001**, *112*, 55.

(19) Covington, A. K.; Paabo, M.; Robinson, R. A.; Bates, R. G. *Anal. Chem*. **1968**, *40*, 700.

(20) Leis, J. R.; Pena, M. E.; Rios, A. *J. Chem. Soc., Chem. Commun*. **1993**, 1298.

(21) Logager, T.; Sehested, K. *J. Phys. Chem*. **1993**, *97*, 6664.

(22) Campestrini, S.; Meunier, B. *Inorg. Chem*. **1992**, *31*, 1999.

Chart 1

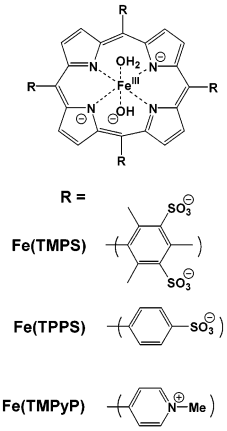

Vinjamoori of the Analytical Sciences Center of Monsanto Corporate Research on a Dionex DX-500 system equipped with an IonPac AS4A-SC column, using bicarbonate-buffered aqueous eluant and suppressed conductivity detection. The amount of charged peroxynitrite was determined spectrophotometrically, and the product ion concentrations were corrected for excess residual nitrite ions (vide supra). Absolute concentrations of authentic nitrite and nitrate ions in control mixtures were accurately quantified.

Catalyst Titrations. In a typical experiment, a sample of Fe(TPPS) (2.8 mg) was dissolved in 500 mL of H_2O to give a 5.0 μM solution. To a 200 mL aliquot was added 40 mg of sodium acetate and 40 μL of acetic acid to provide slight buffer capacity and quantitative formation of the orange bis(aquo) complex at the starting pH. NaOH (1.0 N) and HCl (0.1 N) were added to adjust the pH upward, and spectra were recorded over a 200−700 nm range on a Beckman DU-70 UV−visible spectrophotometer at increasing pH until complete conversion to the green hydroxo(aquo) complex was obtained; change in total solution volume was negligible, and no dilution correction was applied. The Soret band shifted from 393 to 412 nm, and five isosbestic points were observed at 356, 405, 498, 553, and 667 nm. Absorption data obtained at the Soret λ_{max} for both forms were fit to the Henderson−Hasselbalch equation, which indicated that transfer of a single proton had occurred (0.983 H^+ by best fit of limiting absorption, $R^2 = 0.997$), with $pK_1 = 7.10$. The color change was reversed by addition of acid.

Results

General Observations.[12] Synthetic Fe(III) porphyrin complexes, made water-soluble by incorporation of ionic meso substituents (Chart 1), are catalysts for decomposition of peroxynitrite. The presence of micromolar concentrations of these complexes under "physiological conditions" (i.e., pH 7.4, 37 °C) resulted in a significant increase in the decay rate of peroxynitrite above the previously reported background rate. The decay of peroxynitrite was observed by stopped-flow spectroscopy at 302 nm, the absorption maximum of the anion ($\epsilon = 1670\ M^{-1}\ cm^{-1}$) (Figure 1). The decay of peroxynitrite remained monophasic and approximately first-order, even at peroxynitrite stoichiometries in excess of 100:1 against catalyst. Addition of a reducing cosubstrate was not required to obtain the catalysis, and catalyst bleachings were not observed during the peroxynitrite decay.

Simultaneous scanning of the Soret region revealed peroxynitrite-dependent accumulations of an intermediate for each catalyst, which accumulated upon mixing until steady-state concentrations were reached and then relaxed with depletion of peroxynitrite. The intermediates were spectroscopically identical to products of one-electron oxidations of Fe(III) porphyrins by chemical[23] or electrochemical[24] means and were assigned accordingly an oxoiron(IV) structure, $O{=}Fe^{IV}(P)$.[24] Mass and charge balance requires formation of $NO_2^{\bullet}$ equivalents, which could not be observed directly. In the particular case of Fe(TMPS) (Figure 1), the Soret band shifted between 417 nm [Fe(III)] and 422 nm [oxoiron(IV)] with isosbestic points at 418 and 459 nm. By comparison, stoichiometric oxidation of Fe(TMPS) with *m*-chloroperoxybenzoic acid (*m*-CPBA) shifted the Soret band from 417 to 426 nm with identical isosbestic points.

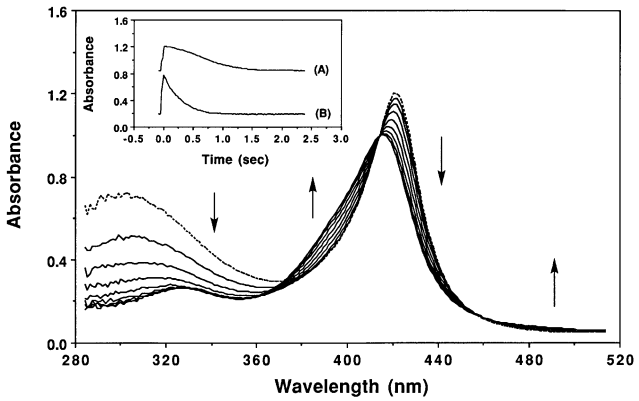

Figure 1. Time-resolved, stopped-flow UV−visible spectra recorded at 32 ms intervals during reaction of Fe(TMPS) (5.0 μM) and peroxynitrite (350 μM). Inset traces illustrate time dependence of absorption at (A) 422 nm, the Soret maximum of oxidized intermediate, and (B) 302 nm, the absorption maximum of $ONOO^-$.

The product anion distribution produced in the presence of the active catalysts, as measured by ion chromatography, was dominated by nitrate. Therefore, the decomposition catalyzed by the Fe(III) porphyrin complexes is predominantly a net isomerization of $ONOO^-$ to NO_3^-.

Reaction Kinetics. Background Decay of Peroxynitrous Acid. Peroxynitrous acid is unstable toward net isomerization to nitrate:[25]

$$ONOO^- + H^+ \underset{K_a}{\overset{\pm H^+}{\leftrightarrow}} ONOOH \xrightarrow{k_1} H^+ + NO_3^- \qquad (1)$$

Minor nitrite yields are attributed to modest competition from disproportionation:[5a,26]

$$ONOOH + ONOO^- \rightarrow 2NO_2^- + O_2 \qquad (2)$$

Rates and products of the background reaction in the absence of catalyst were quantified in order to correct catalytic data and to validate experimental techniques.

(23) (a) Balasubramanian, P. N.; Smith, J. R. L.; Kaaret, T. W.; Bruice, T. C. *J. Am. Chem. Soc.* **1989**, *111*, 1477. (b) Murata, K.; Panicucci, R.; Gopinath, E.; Bruice, T. C. *J. Am. Chem. Soc.* **1990**, *112*, 6072.
(24) (a) Kaaret, T. W.; Zhang, G. H.; Bruice, T. C. *J. Am. Chem. Soc.* **1991**, *113*, 4652. (b) Rodgers, K. R.; Reed, R. A.; Su, Y. O.; Spiro, T. G. *Inorg. Chem.* **1992**, *31*, 2688. (c) Chen, S.-M.; Sun, P.-J.; Su, Y. O. *J. Electroanal. Chem.* **1990**, *294*, 151. (d) Chen, S.-M.; Su, Y. O. *J. Chem. Soc., Chem. Commun.* **1990**, 491.
(25) Kissner, R.; Nauser, T.; Bugnon, P.; Lye, P. G.; Koppenol, W. H. *Chem. Res. Toxicol.* **1997**, *10*, 1285.

Table 1. Catalytic Rate Constants[a]

catalyst	k_{cat} (M^{-1} s^{-1})	k_2/K_m (M^{-1} s^{-1})	k_2 (s^{-1})	K_m (μM)	k_1 (M^{-1} s^{-1})	k_1K_m (s^{-1})
Fe(TMPS)	$3.0(1) \times 10^5$	3.9×10^5	$1.9(5) \times 10^2$	$4.9(6) \times 10^2$	$4.4(4) \times 10^5$	$2.2(3) \times 10^2$
Fe(TPPS)	$8.6(2) \times 10^5$	9.3×10^5	$6(1) \times 10^2$	$6.2(4) \times 10^2$		
Fe(TMPyP)	$1.6(6) \times 10^6$	1.5×10^6	$6(1) \times 10^2$	$3.7(4) \times 10^2$	$>5 \times 10^6$	$>2 \times 10^3$

[a] Data were recorded at pH 7.40, 37.0 °C, 5.0 μM catalyst.

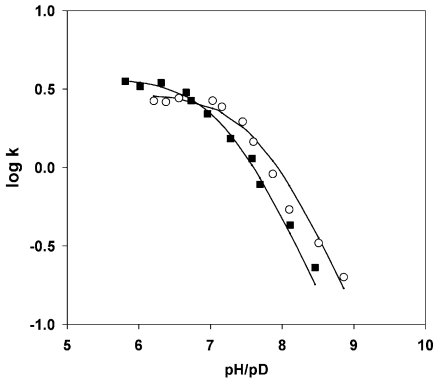

Figure 2. Observed rates of uncatalyzed peroxynitrite decay (350 μM) as a function of solution acidity in H_2O (■) and D_2O (○) at 37 °C.

Observed rates were fit to

$$-\mathrm{d}/\mathrm{d}t([\mathrm{ONOOH}] + [\mathrm{ONOO}^-]) = k_{obs}([\mathrm{ONOOH}] + [\mathrm{ONOO}^-]) \quad (3)$$

where

$$k_{obs} = k_{H^+}[H^+]/([H^+] + K_a) = (\alpha_{HOONO})k_{H^+}$$

(see Figure 2) where k_{H^+} is the limiting decay rate of peroxynitrous acid and K_a is the acid dissociation constant of peroxynitrous acid. Nonlinear least-squares regression produced an excellent fit to eq 3 with $k_{H^+} = 3.73(9)$ s^{-1} and $pK_a = 7.16(4)$. The fitted decay rate of 1.35 s^{-1} at pH 7.40 corresponds to $t_{1/2} = 0.51$ s. These results differ somewhat from an earlier determination, $k_{H^+} = 0.65$ s^{-1} and $pK_a = 7.49$ at 37 °C,[11] but correspond more closely to the results of recent studies, $k_{H^+} = 4.1-4.5$ s^{-1} and $pK_a = 6.7(2)$.[5a,27,28] Also, the kinetic pK_a value can be compared to a spectrophotometrically determined value of 6.5 ± 0.1 near 25 °C.[21]

Measurements of the acid rate dependence also were made in D_2O. Observed rates were faster generally in D_2O, due to alkaline shifts of K_a in the heavy water, $k_{D^+} = 3.0(1)$ s^{-1} and $pK_a = 7.64(9)$; thus $k_{H^+}/k_{D^+} = 1.2(1)$ and $\Delta pK_a = 0.5(1)$, which compares to previous results, $k_{H^+}/k_{D^+} = 1.6(2)$ and $\Delta pK_a = 0.5$.[28]

Reaction Kinetics. Catalyzed Decay of Peroxynitrite. To summarize the general observations above, three primary features of the catalysis can be distinguished: (A) accumulation of oxoiron(IV) catalyst; (B) decay of peroxynitrite, primarily to form nitrate; and (C) return of oxoiron(IV) to the Fe(III) resting state. Each of these was examined separately.

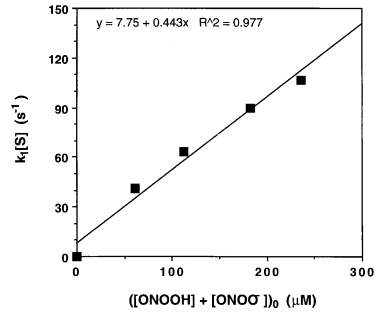

Figure 3. Rates of initial oxidation of Fe(TMPS) (5.0 μM) versus initial peroxynitrite concentration (observed at 422 nm) at pH 7.4, 37 °C.

A. Catalyst Oxidation. Bimolecular rates for oxidation of the Fe(III) porphyrin catalysts by peroxynitrite

$$Fe^{III}(P)^+ + \mathrm{ONOOH/ONOO}^- \rightarrow O{=}Fe^{IV}(P) \quad (4)$$

were determined by monitoring the rates of oxoiron(IV) Soret band accumulations as a function of initial peroxynitrite concentration at pH 7.4. Data obtained for Fe(TMPS) (Figure 3) indicate the reaction rate is first-order in peroxynitrite, $k_{obs} = k_1[\text{peroxynitrite}]_0$; the derived k_1 value is listed in Table 1. Oxidation of Fe(TMPyP) was complete within the flow stop time (ca. 16 ms), even for near-stoichiometric additions of peroxynitrite (ca. 25 μM vs 5 μM), and a lower limit of $k_1 \geq 10^7$ M^{-1} s^{-1} was estimated by assuming $t_{obs} \geq 3t_{1/2}$. Accumulation of oxidized Fe(TPPS) was uniquely biphasic, and the slow second phase showed no dependence on peroxynitrite concentration. This behavior is attributed to cracking of an unreactive oxo-bridged dimer (vide infra). Therefore, an experimental value of the rate constant for Fe(TPPS) oxidation could not be obtained, but it is limited to a range between those of Fe(TMPyP) and Fe(TMPS).

B. Peroxynitrite Decay. Rates of peroxynitrite decay in the catalytic reactions were found to be dependent on concentrations of catalyst and peroxynitrite and on solution acidity. The effects of each of these three variables were quantified independently.

Kinetic Effect of Catalyst Concentration. Rate measurements of peroxynitrite decay were made with catalyst concentrations varying over the range 0−15 μM while initial peroxynitrite concentration (350 μM) and solution pH (7.4) were held constant (Figure 4).

The reactivities of the catalysts varied nearly 10-fold over the order Fe(TMPS) < Fe(TPPS) < Fe(TMPyP). A linear dependence, $k_{obs} = \alpha k_{H^+} + k_{cat}[\text{catalyst}]_0$, was observed for Fe(TMPS) and also for [Fe(TPPS)] < 10 μM. At higher [Fe(TPPS)], a monotonic drop in observed rates below the linear extrapolation at higher concentrations was again attributed to accumulation of unreactive oxo-bridged dimer. In contrast, an upward parabolic rate dependence was obtained for Fe-

(26) Pfeiffer, S.; Gorren, A. C. F.; Schmidt, K.; Werner, E. R.; Hansert, B.; Bohle, D. S.; Mayer, B. *J. Biol. Chem.* **199**7, *272*, 3465.
(27) Koppenol, W. H.; Moreno, J. J.; Pryor, W. A.; Ischiropoulos, H.; Beckman, J. S. *Chem. Rev. Toxicol*. **1992**, *5*, 834.
(28) Padmaja, S.; Kissner, R.; Bounds, P. L.; Koppenol, W. H. *Helv. Chim. Acta* **1998**, *81*, 1201.

Table 2. Limiting Catalytic Rate Constants (Corrected for Equilibria)[a]

catalyst	pK_1[b]	pK_1[c]	pK_a[c]	k_a''' (M^{-1} s^{-1})	k_a'' (M^{-1} s^{-1})	k_b'' (M^{-1} s^{-1})	k_b' (M^{-1} s^{-1})
Fe(TMPS)	8.23	8.5(3)	6.1(2)	$1.4(2) \times 10^6$	$3.1(5) \times 10^6$	$2.6(4) \times 10^5$	
Fe(TPPS)	7.10				3.5×10^6	4.1×10^6	
Fe(TMPyP)	4.73	5.2(7)	6.8(4)		$3.9(8) \times 10^6$	$1.0(9) \times 10^9$	$1.1(2) \times 10^6$
none			7.16(4)				

[a] Data were recorded at 37.0 °C, 5.0 μM catalyst, and fitted to eq 7. [b] Determined by spectrophotometric titration. [c] Determined by fit to kinetic data.

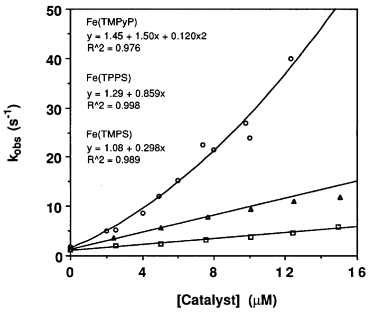

Figure 4. Observed decomposition rates of peroxynitrite (350 μM) versus catalyst concentrations at pH 7.4, 37 °C, as monitored at 302 nm.

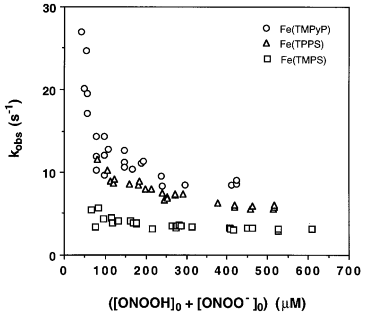

Figure 5. Observed decomposition rates of peroxynitrite decomposition (302 nm) versus initial peroxynitrite concentrations for 5.0 μM catalyst at pH 7.4, 37 °C.

(TMPyP), and a linear tangent was fit to data at [Fe(TMPyP)] $\leq$ 8 μM. The data are summarized in Table 1 (i.e., k_{cat}).

Effects of Peroxynitrite Concentration. Peroxynitrite decay rates also were measured as a function of initial peroxynitrite concentration at fixed catalyst concentration (5.0 μM) and solution pH (7.4). Hyperbolic dependences were found across a ca. 40−610 μM range for all three catalysts (Figure 5). Peroxynitrite decay rates decreased rapidly with increasing peroxynitrite from oxidation limits to reach nearly constant plateaus, which are defined by k_{cat} and tend downward toward zero at infinite peroxynitrite concentrations. The order of catalyst activities, Fe(TMPS) < Fe(TPPS) < Fe(TMPyP), was maintained over the entire range.

Initial velocity data, when corrected for background decay, were found to fit Michaelis−Menten kinetics (vide infra) (Figure 6). Values of K_m (i.e., the "dissociation" constant of the catalyst−substrate complex), and k_2 (i.e., the limiting turnover rate of the complex) were obtained from the Lineweaver−Burk plots. These values are listed in Table 1, along with calculated bimolecular catalytic rate constants (i.e., $k_{cat} = k_2/K_m$) and total dissociation rates for the catalyst−substrate complexes (i.e., $k_{-1} + k_2 = k_1K_m$).

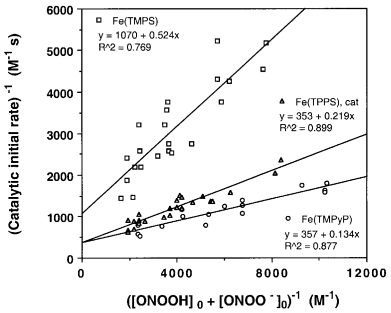

Figure 6. Lineweaver−Burk plots of inverse initial rates versus inverse initial peroxynitrite concentration (the data are taken from runs plotted in Figure 5 and corrected for background peroxynitrite decay).

Effects of Solution pH: Catalyst Equilibria. The Fe(III) porphyrins undergo acid-dependent equilibria[29]

$$(H_2O)Fe^{III}(P)(OH_2)^+ \underset{K_1}{\overset{\pm H^+}{\longleftrightarrow}} (HO)Fe^{III}(P)(OH_2) \underset{K_2}{\overset{\pm H^+}{\longleftrightarrow}} (HO)Fe^{III}(P)(OH)^- \quad (5)$$

and the various catalyst forms may differ in reaction rates with peroxynitrite. Independent values of K_1 were obtained by routine spectrophotometric titrations (Table 2). Accumulations of bis(hydroxo) complexes via K_2 were not observed under any relevant conditions. The data clearly reflect the differing charges of the meso substituents (Chart 1).

The (aquo)(hydroxo) catalyst forms undergo an additional, pH-independent equilibrium to form an unreactive oxo-bridged dimer:

$$2(HO)Fe^{III}(P)(OH_2) \overset{K_d}{\longleftrightarrow} (H_2O)(P)Fe^{III}-O-Fe^{III}(P)(OH_2) \quad (6)$$

Dimerization of Fe(TMPS) is assumed to be negligible, $K_d \approx 0$, due to steric congestion. Literature K_d values indicate that dimerization can be neglected under all conditions employed in this study for Fe(TMPyP) also and for [Fe(TPPS)] $\leq$ 10 μM at pH 7.4.[29]

Effects of Solution pH: Kinetics. Rates of Fe(TMPS)- and Fe(TMPyP)-catalyzed peroxynitrite decay were measured as a function of solution pH over the range 5.8−8.5 at fixed catalyst (5.0 μM) and peroxynitrite (350 μM) concentrations and at fixed ionic strength (190 mM) (Figures 7 and 8). Similar measurements for Fe(TPPS) were omitted due to oxo-bridged dimer formation. The complex rate−pH profiles reflect the acid-dependent equilibria of peroxynitrite (eq 1) and the catalysts (eq 5), which give rise to multiple oxidation

(29) Miskelly, G. M.; Webley, W. S.; Clark, C. R.; Buckingham, D. A. *Inorg. Chem.* **1988**, *27*, 3773, and references therein.

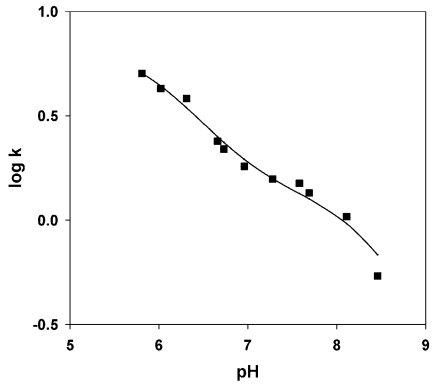

Figure 7. Catalyzed rates for decomposition of peroxynitrite (350 μM) observed at 302 nm versus solution pH for 5.0 μM Fe(TMPS) at 37 °C. Data are fitted to the paths delineated in Scheme 1 after correction for background decay.

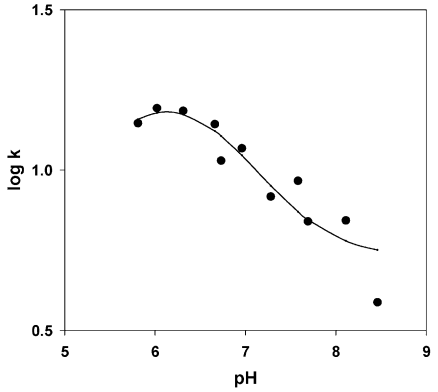

Figure 8. Catalyzed rates for decomposition of peroxynitrite (350 μM) observed at 302 nm versus pH for 5.0 μM Fe(TMPyP) at 37 °C. Data are fitted to the paths delineated in Scheme 1 after correction for background decay.

pathways (Scheme 1). The data were fit to Scheme 1 and

$$k_{obs} = (1 - \alpha_{Fe-OH})[(1 - \alpha_{ONOO^-})k_a''' + (\alpha_{ONOO^-})k_b''] + \alpha_{Fe-OH}[(1 - \alpha_{ONOO^-})k_a'' + (\alpha_{ONOO^-})k_b'] + \alpha_{Fe-OH}(K_2/[H^+])(1 - \alpha_{ONOO^-})k_a' \quad (7)$$

where $[H^+] \gg K_2$, $\alpha_{Fe-OH} = K_1/(K_1 + [H^+])$, and $\alpha_{ONOO^-} = K_a/(K_a + [H^+])$ with the assumption of invariant k_1/k_{cat} ratios across the pH range. Rapid proton transfer prevents distinction of k_b'' reactions of the bis(aquo) catalysts with peroxynitrite anion and k_a'' reactions of the (aquo)(hydroxo) forms with peroxynitrous acid. Therefore, fits to eq 7 were simplified greatly by calculating limiting cases where only the path corresponding to reaction of the dominant catalyst acid form is taken to be significant. Least-squares regression returned values for two dissociation constants (K_a, K_1) and two rate constants (k_a'' or k_b'', and k_b' or k_a'''), Table 2. The opposing k'' limit was obtained from the relation $k_a''/k_b'' = K_a/K_1$. Similar calculations for k_a' values were omitted, since no estimates of K_2 were available.

The fits revealed dominant k'' contributions near pH 7.4. The reactivity of ONOOH was verified by observation of a significant Fe(TMPS) k''' path, 1.4(2) × 10^6 M^{-1} s^{-1}, on which the oxidant must be protonated. However, fitting of this manifold was difficult, as it was severely convoluted

Scheme 1

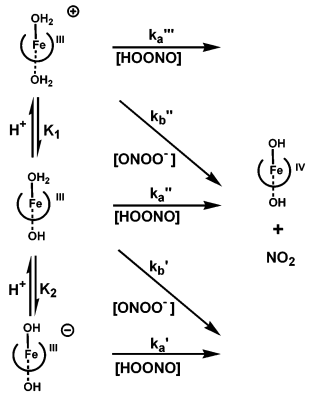

with the k'' and background rates, so that estimates of K_a and k_a''' may contain uniquely large errors. Concordant assignment of the k'' paths to a predominant k_a'' reaction of (aquo)(hydroxo) complexes with ONOOH yields strikingly coincident k_a'' rates for all three catalysts, (3.5 ± 0.4) × 10^6 M^{-1} s^{-1}, Table 2. Fe(TMPyP) would give the fastest catalysis because the positively charged meso substituents facilitate deprotonation of an aquo ligand to give the reactive $(H_2O)Fe^{III}(P)(OH)$ catalyst form.

Solvent Isotope Effects. Measurements of the solution acidity rate dependence were also made for Fe(TMPS) and Fe(TMPyP) in D_2O. The dominant k'' pathways displayed insignificant solvent kinetic isotope effects, $k''_{H^+}/k''_{D^+} = 0.9$-(2) for Fe(TMPS) and $k''_{H^+}/k''_{D^+} = 1.0(5)$, $k'_{H^+}/k'_{D^+} = 1.0$-(4) for Fe(TMPyP); proton transfer probably is absent in the oxidative transition state of the k'' path. In contrast, the Fe-(TMPS) k''' path might exhibit an isotope effect, $k'''_{H^+}/k'''_{D^+} = 2(1)$.

C. Termination of Catalysis and Reductive Catalyst Relaxation. The oxidized catalyst intermediates were observed to return without bleaching to the initial Fe(III) state upon exhaustion of peroxynitrite (Figure 1). These terminal reductions could be fit to first-order decay curves, and the observed rate depended on both the *initial* concentration of peroxynitrite and its decay rate. For example, data for the Fe(TMPS) intermediate were taken from the Michaelis−Menten experiments, and the decay rate increased from zero toward an asymptotic limit with increased initial peroxynitrite concentrations (Figure 9). These observations are consistent with steady-state equilibrium relaxation to the Fe(III) resting state with exhaustion of substrate and not with a terminal reduction, which requires a linear dependence.

Effects of Exogenous Reductants. To elucidate the nature of the oxoiron(IV) reduction, a control reaction was performed between oxidized Fe(TMPS) and nitrite anion (NO_2^-). In a double mixing stopped-flow experiment, the Fe(III) complex was oxidized with *m*-CPBA in the initial mix and varying nitrite concentrations were introduced after a controlled delay.[30] The $O{=}Fe^{IV}$(TMPS) was stable in the absence of nitrite, and reduction to the Fe(III) species was first-order in added nitrite; a rate constant of 2.7(2) × 10^4

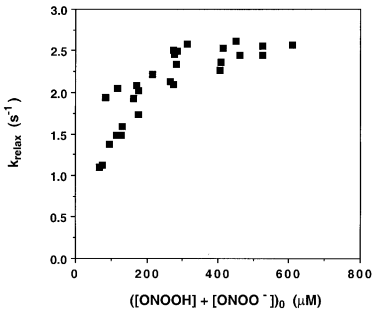

Figure 9. Observed rates of terminal relaxation of O═Fe^{IV}(TMPS) (422 nm) versus initial peroxynitrite concentration at pH 7.4, 37 °C, and 5.0 μM total catalyst.

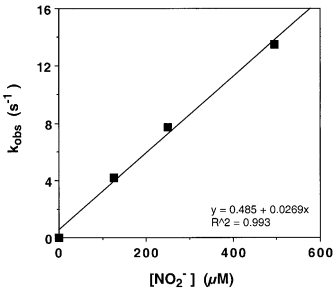

Figure 10. Reduction rates of O═Fe^{IV}(TMPS) (5.0 μM, obtained from *m*-CPBA oxidation) versus nitrite concentration at pH 7.4, 37 °C, observed at 426 nm.

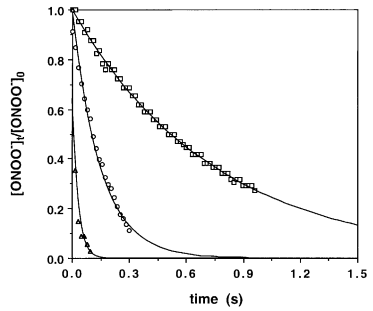

Figure 11. Decay of peroxynitrite (450 μM) observed (302 nm) with added (□) ascorbate (600 μM); (○) Fe(TMPyP) (5.0 μM); or (△) both ascorbate and Fe(TMPyP).

M^{-1} s^{-1} was obtained (Figure 10). Given [NO_2^-] < 100 μM in catalytic reaction mixtures, this rate constant is too slow by a factor of 10^2 to accommodate continuous reductive turnover during catalysis.

In contrast to nitrite, ascorbic acid is known to be a potent scavenger of high-valent metalloporphyrins[30] and also is unreactive with peroxynitrite directly (k_{obs} = 220 M^{-1} s^{-1}).[31] Addition of 600 μM ascorbate was adequate to hold Fe(TMPS) and Fe(TMPyP) in the Fe(III) state throughout catalysis at pH 7.4, which was accelerated strongly to limiting oxidation rates (i.e., k_1) (Figure 11). Product ion concentrations were redirected toward nitrite in the presence of ascorbate (Table 3).

(30) (b) Groves, J. T.; Lee, J.; Marla, S. S. *J. Am. Chem. Soc.* **1997**, *119*, 6269.

(31) (a) Bartlett, D.; Church, D. F.; Bounds, P. L.; Koppenol, W. H. *Free Radicals Biol. Med.* **1995**, *18*, 85. (b) Squadrito, G. L.; Jin, X.; Pryor, W. A. *Arch. Biochem. Biophys.* **1995**, *322*, 53.

Table 3. Ascorbate Effect on Catalysis[a]

	[ascorbate]$_0$ = 0		[ascorbate]$_0$ = 600 μM	
catalyst	k_{cat}[b] (M^{-1} s^{-1})	[NO_2^-][c]	k_{cat}[b] (M^{-1} s^{-1})	[NO_2^-][c]
Fe(TMPyP)	1.6×10^6	0.19 ± 0.12	1×10^7	0.62 ± 0.05
Fe(TMPS)	3.0×10^5		4.3×10^5	
blank buffer	0	0.22 ± 0.16	2.2×10^2	0.46 ± 0.15

[a] 5.0 μM catalyst, pH 7.40, 37.0 °C. [b] 450 μM peroxynitrite. [c] Mole fraction of product ions, 600 mM peroxynitrite.

Discussion

The results described above indicate that the catalyzed peroxynitrite decomposition is an isomerization to nitrate that is mediated by one-electron redox chemistry of the Fe(III) catalysts. Correction of the observed rates for protonation equilibria of the catalysts and peroxynitrite gives coincident limiting rates for all three catalysts, which suggests a common mechanism. The kinetically dominant manifold under "physiological conditions" (pH 7.4, 37 °C) can be assigned to rate-limiting reaction of (aquo)(hydroxo) catalyst tautomers, $(H_2O)Fe^{III}(P)(OH)$ and peroxynitrous acid. Accordingly, the Fe(TMPyP) catalyst has the highest k_{cat} value because the positively charged *meso*-pyridinium substituents favor deprotonation of one axial aquo ligand to form a stronger hydroxo anion donor ligand. The absence of a significant solvent kinetic isotope effect indicates a lack of proton transfer at the oxidative barrier, and this is consistent with displacement of a water ligand by peroxynitrous acid, which is followed by rapid homolysis of the incipient $(ONOOH)Fe^{III}(P)(OH)$ complex. Self-sufficient closure of the redox cycle indicates an endogenous reductant is formed, although exogenous reagents can be added to accelerate catalysis. Control experiments indicate that nitrite is not kinetically competent to serve as the reductant.

The catalytic peroxynitritase reactions were observed to obey Michaelis−Menten kinetics, resulting from the minimal reaction scheme of

$$E + S \underset{k_{-1}}{\overset{k_1}{\rightleftarrows}} ES \xrightarrow{k_2} E + P \qquad (8)$$

The resting Fe(III) catalyst (E) is oxidized reversibly by peroxynitrite substrate (S) to an intermediate state (ES) that turns over irreversibly to product (P = NO_3^-). Substrate turnover is governed by the steady-state rate law of eq 9,[32] which gives first-order behavior, eq 10, at nonsaturating substrate concentrations, [S] < K_m:

$$-d[S]/dt = k_1k_2[S][E]_0/(k_1[S] + k_{-1} + k_2) = k_2[S][E]_0/(K_m + [S]) \qquad (9)$$

$$-d[S]/dt = k_1k_2[E]_0[S]/(k_2 + k_{-1}) = (k_2/K_m)[E]_0[S] = k_{cat}[E]_0[S] = k_{obs}[S] \qquad (10)$$

Experimental values of K_m and k_2 determined from a linear plot of inverse velocity against inverse substrate concentration (Lineweaver−Burk plot), and k_1 was determined from

(32) Conners, K. *Chemical Kinetics*; VCH: New York, 1990; pp 100−105.

the substrate dependence on the rate of initial ES accumulation. Values of k_{cat} were measured directly by the dependence of catalyst concentration on peroxynitrite decay under conditions where eq 10 is valid. Comparison of independent data from the direct k_{cat} and Michaelis−Menten experiments reveal excellent agreement, Table 1.

What are the natures of the ES catalytic intermediate and the k_1, k_{-1}, and k_2 reaction steps? These can be considered by analogy to heme peroxidases, which detoxify hydroperoxides (HOOR) through oxidoreductase catalysis, eqs 11−15:[33]

$$Fe^{III}(P)^+ + HOOR \rightarrow O{=}Fe^{IV}(P^{\bullet +}) + ROH \quad (11)$$

$$O{=}Fe^{IV}(P^{\bullet +}) + AH_2 \rightarrow O{=}Fe^{IV}(P) + AH \quad (12)$$

$$O{=}Fe^{IV}(P) + AH_2 \rightarrow Fe^{III}(P)^+ + AH \quad (13)$$

$$2AH \rightarrow AH_2 + A \quad (14)$$

$$\text{net:} \qquad ROOH + AH_2 \rightarrow ROH + A + H_2O \quad (15)$$

Reducing substrates (AH_2) reduce compound I, $O{=}Fe^{IV}(P^{\bullet +})$, and compound II, $O{=}Fe^{IV}(P)$, intermediates back to the Fe(III) resting state. The second reduction typically is much slower, due to lower driving force and greater reorganization required to quench the iron(IV)oxo compared to the porphyrin radical, so that the compound II state frequently is the only observed intermediate.

Observed spectra of the ES intermediates in this work are identical to those of electrochemically generated compound II states, $O{=}Fe^{IV}(P)$. However, mass and charge balances require formation of an undetected $NO_2^{\bullet}$ radical. Together, the oxoFe(IV) complex and nitrogen dioxide comprise a bimolecular analogue of compound I, in which the oxidizing equivalent on $NO_2^{\bullet}$ is stabilized relative to the porphyrin ligand (i.e., $[O{=}Fe^{IV}(P), NO_2^{\bullet}]$ vs $[O{=}Fe^{IV}(P^{\bullet +}), NO_2^-]$). Oxidation to the ES state could occur directly by homolysis of Fe(III) peroxide to form $[O{=}Fe^{IV}(P), NO_2^{\bullet}]$ or by heterolysis to form $[O{=}Fe^{IV}(P^{\bullet +}), NO_2^-]$, with a fast subsequent electron transfer. However, dissociation of ES along the microscopic reverse (i.e., k_{-1}) is obtainable only for a homolytic oxidation.

Since a reducing cosubstrate (AH_2) is not required for catalysis, identification of the endogenous reductant is required to complete the peroxidase analogy, eq 15. The obvious candidate is nitrite, which is formed by the known hydrolytic disproportionation of nitrogen dioxide:

$$2NO_2^{\bullet} \leftrightarrow N_2O_4 \quad (16)$$

$$N_2O_4 + H_2O \rightarrow NO_2^- + NO_3^- + 2H^+ \quad (17)$$

Reduction of $O{=}Fe^{IV}(P)$ by nitrite produces a second equivalent of $NO_2^{\bullet}$, and disproportionation produces nitrate product and replaces the consumed nitrite:

$$Fe^{III}(P) + ONOOH \rightarrow [O{=}Fe^{IV}(P), NO_2^{\bullet}] \quad (18)$$

$$[O{=}Fe^{IV}(P), NO_2\bullet] + NO_2^- \rightarrow [Fe^{III}(P), NO_2^{\bullet}] + NO_2^{\bullet} \quad (19)$$

$$2NO_2^{\bullet} \rightarrow NO_2^- + NO_3^- \quad (20)$$

$$\text{net:} \qquad ONOOH \rightarrow NO_3^- \quad (1)$$

Reduction by an exogenous equivalent of $NO_2^{\bullet}$ yields the alternative scheme:

$$Fe^{III}(P) + ONOOH \rightarrow [O{=}Fe^{IV}(P), NO_2^{\bullet}] \quad (18)$$

$$[O{=}Fe^{IV}(P), NO_2^{\bullet}] + NO_2^{\bullet} \rightarrow [O{=}Fe^{IV}(P), NO_2^-] + NO_3^- \quad (21)$$

$$[O{=}Fe^{IV}(P), NO_2^-] \rightarrow Fe^{III}(P) + NO_2^{\bullet} \quad (22)$$

$$\text{net:} \qquad ONOOH \rightarrow NO_3^- \quad (1)$$

in which the disproportionation effects reduction of the compound I pair to compound II, $[O{=}Fe^{IV}(P), NO_2^{\bullet}]$ to $[O{=}Fe^{IV}(P), NO_2^-]$, and releases a product nitrate ion. Subsequent rearrangement of compound II completes the turnover by releasing resting catalyst $Fe^{III}(P)$ and replacing the consumed equivalent of $NO_2^{\bullet}$.

Unfortunately, neither of the above possibilities is satisfactory. First, a mechanism for the k_{-1} path is not apparent. Reduction of $O{=}Fe^{IV}(P)$ by nitrite is required in both cases, which was demonstrated independently to be 10^2 slower than the catalytic turnover. Literature values[34,35] for rate constants of the $2NO_2^{\bullet}/N_2O_4$ equilibrium ($k_{16} = 4.5 \times 10^8\ M^{-1}\ s^{-1}$, $k_{-16} = 6.9 \times 10^3\ s^{-1}$, $K_{16} = 6.5 \times 10^4\ M^{-1}$) and N_2O_4 hydrolysis ($k_{17} = 1 \times 10^3\ s^{-1}$) indicate the extent of $NO_2^{\bullet}$ dimerization is modest (31% $NO_2^{\bullet}$ dimerized at 5 μM oxidized catalyst), and as a result, the calculated rate of $NO_2^{\bullet}$ decay is relatively slow ($<200\ s^{-1}$ at 5 μM oxidized catalyst) compared to reduction of oxidized catalyst ($k_{-1} + k_2$, Table 1).

The major reductant is therefore assigned as $NO_2^{\bullet}$ itself. The observed intermediates are $[O{=}Fe^{IV}(P), NO_2^{\bullet}]$ compound I states, which collapse directly to Fe(III) porphyrin by direct inner-sphere combination with transfer of the Fe(IV) oxo atom. The resulting catalytic manifold is summarized in Scheme 2. The inner-sphere mechanism circumvents the typically slow outer-sphere electron transfer of $O{=}Fe^{IV}(P)$ by O-atom transfer. The radical character (i.e., the singly occupied HOMO) of $NO_2^{\bullet}$ extends over all three atoms, and the bimolecular combination should yield either nitrate or peroxynitrite, thus affording both k_{-1} and k_2 reductive paths in a simple partition of a single physical event. This resembles both the radical mechanism for self-isomerization of peroxynitrite[5] and the "oxygen rebound" mechanism of the cytochromes P_{450}.[36]

(33) Valentine, J. S. In *Bioinorganic Chemistry*; Bertini, I., Gray, H. B., Lippard, S. J., Valentine, J. S., Eds.; University Science: Mill Valley, CA, 1994; Chapt. 5, pp 295−298.

(34) Ottolenghi, M.; Rabani, J. *J. Phys. Chem.* **1968**, *72*, 593.

(35) (a) Graetzel, M.; Henglein, A.; Lillis, J.; Beck, G. *Ber. Bunsen-Ges. Phys. Chem.* **1969**, *73*, 627. (b) Treinin, A.; Hayon, E. *J. Am. Chem. Soc.* **1970**, *92*, 5821.

(36) Groves, J. T. *J. Chem. Educ.* **1985**, *62*, 928.

Scheme 2

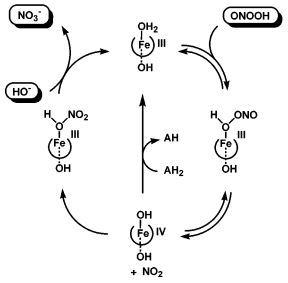

Pulse radiolysis experiments demonstrate that combination of $NO_2^\bullet$ and $HO^\bullet$ radicals is diffusion-controlled and yields both peroxynitrite and nitrate;[21,37] an analogy is thus drawn between $^\bullet OH$ and $O{=}Fe^{IV}(P)$ [i.e., between $^\bullet OH$ and $^\bullet O{-}Fe^{III}(P)$]. Photolysis in benzene of the nitrato complex of tetraphenylporphyrinato iron(III) produces $NO_2^\bullet$ and the oxoiron(IV) complex,[38] in reverse of the thermal k_2 step here. Similar trapping of $NO_2^\bullet$ in aqueous solution can be obtained in competition with hydrolysis by reduction from 10^{-5} M ferrocyanide.[34] Thus, while the recombination was not demonstrated directly, there is ample reason to extend consideration to this reaction as a mechanism for catalyst turnover.

The proposed $NO_2^\bullet$ capture at oxoiron(IV) requires a bimolecular ES state in the absence of strong cage effects, and this has implications for the Michaelis−Menten kinetics. Thus, eqs 9 and 10 are rewritten (e.g., $k_2 = k_2'[NO_2^\bullet]$) as

$$-\mathrm{d[S]}/\mathrm{d}t = k_1k_2'[NO_2^\bullet][S][E]_0/(k_1[S] + k_{-1}'[NO_2^\bullet] + k_2'[NO_2^\bullet])$$

$$= k_2'[NO_2^\bullet][S][E]_0/(K_m' + [S]) \qquad (23)$$

$$-\mathrm{d[S]}/\mathrm{d}t = k_1k_2'[NO_2^\bullet][E]_0[S]/(k_2' + k_{-1}')[NO_2^\bullet] \qquad [S] < K_m$$

$$= (k_2'/K_m')[E]_0[S] = k_{cat}[E]_0[S] = k_{obs}[S] \qquad (24)$$

to account for bimolecular turnover. The forms of eqs 10 and 24 are identical, and both predict the observed linear dependence of catalyst concentration on peroxynitrite decay; cage effects are irrelevant. Observed turnover rates (Table 1) require that $k_2' = 10^8\ M^{-1}\ s^{-1}$. However, turnover-limited kinetics at high peroxynitrite concentrations would then conform to

$$-\mathrm{d[S]}/\mathrm{d}t = k_2'[NO_2^\bullet][E]_0 = k_2'[E]_0^2 \qquad (25)$$

and the catalysis tends toward second-order catalyst dependence. This effect will be most pronounced at low concentrations of the fastest catalysts (i.e., with the largest k_1 values). Indeed, parabolic curvature is observed for k_{cat} plots of the Fe(TMPyP)-catalyzed reaction at low catalyst concentration (Figure 4). The plot tends toward linearity at higher concentration, presumably as the bimolecular reduction becomes increasingly competitive.

Chart 2

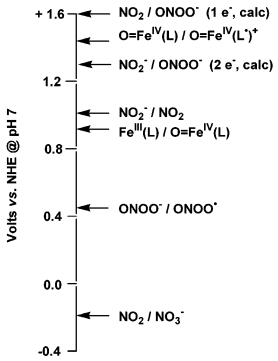

Addition of ascorbate (AH_2) is predicted to trap oxoiron(IV) species, which increases the catalyst turnover rate

$$k_2 = k_2'[NO_2^\bullet] + k_2''[AH_2] \qquad (26)$$

and shifts the steady-state catalyst equilibrium toward the Fe(III) resting state (i.e., $K_m \rightarrow \infty$ as $[AH_2] \rightarrow \infty$). Disposal of $NO_2^\bullet$ occurs by hydrolysis or ascorbate reduction, which shifts the product ion distribution toward nitrite, $0.5[\text{peroxynitrite}]_0 \le [NO_2^-]_\infty \le 1.0[\text{peroxynitrite}]_0$, in accord with experimental observations (Table 3).

Finally, the thermodynamic feasibility of the proposed oxidoreductase catalysis can be assessed, as one- and two-electron aqueous oxidation potentials are available for Fe(III) porphyrins,[24] peroxynitrite,[5a,27] and various nitrogen oxides[5a,27] (Chart 2). The data indicate strong driving forces for one-electron chemistry for both the oxidative and reductive half-reactions; the Fe(III)/O=Fe(IV) potential is well placed between the one-electon potentials peroxynitrite reduction (to $NO_2^\bullet$), and $NO_2^\bullet$ oxidation (to NO_3^-). In the event of $NO_2^\bullet$ hydrolysis, peroxynitrite anion also would be suitable as a secondary one-electron reductant; this sequence would give the minor nitrite yields (eqs 2 and 17). Nitrite would offer little or no driving force.

Conclusions

These results further document and define the fast peroxynitrite isomerization catalysis afforded by water-soluble Fe(III) porphyrins. Observed reaction rates with peroxynitrite approach $10^7\ M^{-1}\ s^{-1}$, which are among the highest known for bimolecular reactions of peroxynitrite. Catalyst concentrations of 10^{-5} M are adequate to completely outstrip the background decay.

Despite the rapidity of the peroxynitrite isomerization catalysis, it is probably irrelevant under actual physiological conditions. Concentrations of peroxynitrite attainable in vivo fall well below the K_m values obtained here, while concentrations of ascorbate (e.g., 1.0 mM),[31] are adequate to push the metalloporphyrin-mediated reductase catalysis to the oxidation limit. Direct reactions of antioxidants with peroxynitrite typically are quite slow.[39] The predicted effect of the

(37) Merenyi, G.; Lind, J.; Goldstein, S.; Czapski, G. *J. Phys. Chem. A* **1999**, *103*, 5685.
(38) Suslick, K. S.; Watson, R. A. *Inorg. Chem.* **1991**, *30*, 912.
(39) Lymar, S.; Hurst, J. K. *Chem. Res. Toxicol.* **1996**, *9*, 845.

iron porphyrins in vivo would be to catalyze rapid reduction of peroxynitrite by an otherwise unreactive antioxidant pool,[30] thus suppressing the oxidative component of any peroxynitrite pathology. In essence, the catalysis replaces an indiscriminant oxidant ($HO^{\bullet}$) with $O{=}Fe^{IV}(P)$, which reacts selectively with one-electron antioxidant couples.

Although the biochemical effects of peroxynitrite remain to be elucidated fully,[40−42] the results of this study are consistent with suggestions that peroxynitrite scavenging might account for the observed pharmacological efficacy of synthetic metalloporphyrins in disease models of oxidative stress injury.[18]

Finally, it is noteworthy that the general kinetic features of alkyl hydroperoxide reductions by Fe(III) porphyrins, particularly pH dependences and solvent isotope effects,[43] are retained in the peroxynitrite isomerization catalysis, albeit at 10^4-fold higher rates.

Acknowledgment. This work was supported by Monsanto. We thank Dr. Michael K. Stern of Monsanto for preliminary work and advice and Professors Daryle Busch (Kansas), John Groves (Princeton), and Jack Halpern (Chicago) for helpful consultations.

Supporting Information Available: Data for spectrophotometric acid titrations of Fe(III) porphyrin catalysts, spectra of *m*-CPBA oxidation of Fe(TMPS), and tables of kinetic data. This material is available free of charge via the Internet at http://pubs.acs.org.

IC011089S

(40) (a) van der Vliet, A.; Eiserich, J. P.; Halliwell, B.; Cross, C. E. *J. Biol. Chem*. **1997**, *272*, 7617. (b) Eiserich, J. P.; Milena, H.; Cross, C. E.; Jones, A. D.; Freeman, B. A.; Halliwell, B.; van der Vliet, A. *Nature* **1998**, *391*, 393.

(41) Fukuto, J. M.; Ignarro, L. J. *Acc. Chem. Res*. **1997**, *30*, 149.

(42) Pfeiffer, S.; Schrammel, A.; Koesling, D.; Schmidt, K.; Mayer, B. *Mol. Pharmacol*. **1998**, *53*, 795.

(43) (a) Lindsay Smith, J. R.; Lower, R. J. *J. Chem. Soc., Perkin Trans. 2* **1991**, 31. (b) Gopinath, E.; Bruice, T. C. *J. Am. Chem. Soc*. **1991**, *113*, 4657 and 6090. (c) Culclough, N.; Lindsay Smith, J. R. *J. Chem. Soc., Perkin Trans. 2* **1995**, 235.